Comparative Study of Bioleaching Efficiency of Rare Earth Element from Different Carbonatite Ores in Mongolia

Bayarbayasgalan Bayarsaikhan[1], Altangerel Amarsanaa[1*], Purevjargal Daramjav[1], Hongbo Zhao[2], Sarangerel Davaasambuu[1]

[1]Department of Chemistry, Division of Natural Sciences, School of Arts and Sciences, National University of Mongolia, Ulaanbaatar, 14201, Mongolia
[2]School of Minerals Processing and Bioengineering, Central South University, Changsha, 410083, China

Abstract: The increasing demand for rare earth elements necessitates the development of environmentally friendly and energy-efficient extraction methods. This study investigates the bioleaching efficiency of rare earth elements from carbonatite ores using both pure and mixed bacterial cultures under ambient conditions. Ores from the Lugiin Gol and Mushgia Khudag deposits underwent a 7-day bioleaching with a bacterial mixture and pure cultures origin from copper ore. The progress of bioleaching was monitored by measuring dissolved metal concentrations, pH, and oxidation-reduction potential. X-ray diffraction analysis revealed that rare earth elements predominantly exist as minerals synchysite and bastnasite in the Lugiin Gol ore, monazite and parasite in the Mushgia Khudag ore. Chemical analysis determined the total REE content to be 3.99% in Lugiin Gol ore and 7.66% in Mushgia Khudag ore. The bioleaching, conducted with a solid-to-liquid ratio of 1:6 at room temperature and utilizing six different ore particle sizes, demonstrated that mixed bacterial cultures were significantly more effective than pure cultures. The highest metal recovery rates achieved were 15.85% and 6.23% (wt.%) for Lugiin Gol and Mushgia Khudag ores, respectively. Furthermore, particle size was identified as a crucial factor influencing bioleaching efficiency, with optimal results observed at 4.0–5.0 mm particle sizes, likely due to the weakening of the rare earth element bearing ore matrix.
Keywords: monazite, synchysite, bacterial leaching, mixed bacteria, metal recovery, particle size

1. Introduction

Bioleaching is an environmentally friendly, simple, and cost-effective method, making it an attractive green technology for the extraction and recovery of metals from ores. It has been successfully employed for extracting metals like copper (Santaolalla, Gutierrez, Gallastegui, Barona, & Rojo, 2021; Watling, 2006a), nickel (Halinen, Rahunen, Kaksonen, & Puhakka, 2009; Hosseini Nasab, Noaparast, Abdollahi, & Amoozegar, 2020), zinc (Rodríguez, 2003; Zahiri, Ahmadi, Foroutan, & Ghadiri, 2021), and rare earth elements (REEs) (Ma et al., 2023; Shen et al., 2023) from dispersed low-grade ores, with recovery rates ranging from 59% Ni to 90% Cu. Recent research has focused on the isolation of microorganisms capable of selectively leaching specific metals, with a particular emphasis on the bioleaching of REEs, often called the "vitamins of industry" due to their importance in high-tech applications.

REEs are commonly found in carbonatite rocks, weathered alkaline igneous rocks, and ion-exchange clays (Dostal & Gerel, 2023; Liu et al., 2023), with approximately 53.6% of the known REEs reserves occurring in carbonatites, primarily in minerals such as bastnäsite, synchysite, parisite, and monazite (Liu et al., 2023). Conventional methods for REEs extraction from carbonatite ores, including thermal pretreatment followed by concentrated acid leaching or direct acid/alkali leaching, achieve metal recovery of 77.0%-92.0% for Ce and Nd (Feng et al., 2013; Huang, Dou, Zhang, & Liu, 2017; Huang, Zhang, Dou, Liu, & Tang, 2014). However, these methods are costly (Zhang et al., 2018), energy-intensive (Shen et al., 2023), and environmentally damaging (Owusu-Fordjour & Yang, 2023; Shen et al., 2023).

Given these challenges, the exploration of bioleaching as an alternative for REEs extraction from ores has gained momentum. Bioleaching agents include both fungi and bacteria. Fungi such as *Aspergillus niger* (Brisson, Zhuang, & Alvarez-Cohen, 2016; Shen et al., 2023; Su, Chen, & Lin, 2020), *Aspergillus terreus* (Brisson et al., 2016), *Yarrowia lipolytica* (Shen et al., 2023), and *Penicillium* sp. (Gonzalez Baez, Muñoz, Timmermans, Garelick, & Purchase, 2024; Qu & Lian, 2013) have been extensively studied for REEs bioleaching. Among bacteria, gram-negative *Enterobacter, Acidithiobacillus* (Fathollahzadeh et al., 2018) and *Pseudomonas* (Shin, Kim, Kim, Jeong, & Lee, 2015) are the most researched for REEs extraction from monazite-rich ores.

Monazite, a phosphate-rich REE mineral, is often bioleached using phosphate-solubilizing microorganisms. For instance, *Pseudomonas rhizosphaerae*, *Bacillus megaterium*, and *Acetobacter aceti* have been used to bioleach monazite ore containing high concentrations of lanthanum (3.5%) and cerium (2.09%). Among these *Pseudomonas rhizosphaerae* was the most effective for lanthanum, while *Acetobacter aceti* showed highest efficiency for cerium, achieving relatively low metal recovery of 0.11%, and 0.13%, respectively (Shin et al., 2015). Similarly, Corbett et al. (2024) used a combination of heterotrophic microbial species, including *Klebsiella aerogenes*, *Burkholderia T48*, *Acacia stenophylla*, and *Pseudomonas putida* to bioleach REEs from high-grade monazite. They varied the carbon source (galactose, fructose, or maltose) during the bioleaching process. Fructose led to the highest organic acid production by the mixed microorganisms and the greatest rare earth element leaching, reaching approximately 1400 µg/L (Corbett, Gifford, Fimognari, & Watkin, 2024).

While several studies have focused on the biological leaching of monazite-containing REE ores, limited research has been conducted on the bioleaching of carbonatite ores containing bastnasite and synchysite. Zhang (2018) isolated different species of actinobacteria from rare earth element bearing carbonatite ores and surrounding soil, achieving REEs leaching rates of 56-342 µg/L over 20 days. Among them, *Streptomyces* sp. grown in an oligotrophic media, exhibited the highest leaching efficiency, reaching 548 µg/L from bastnasite.

Although thiobacteria are commonly used for sulfide ore bioleaching, they have also been employed in REEs leaching. For instance, *Acidithiobacillus ferrooxidans* was used to leach spent fluid catalytic cracking catalysts, achieving metal recovery rates of 83% for lanthanum and 23% for cerium (Muddanna & Baral, 2021). Additionally, Fathollahzadeh et al. (2018) demonstrated the synergistic effect of combining autotrophic *Acidithiobacillus ferrooxidans* and heterotrophic *Enterobacter aerogenes* in bioleaching monazite ore, achieving a 1.28% total REE recovery due to the production of sulfuric and organic acids including gluconic, acetic, and malic acid, during microbial metabolism.

However, despite progress, the overall recovery of REEs via bacterial leaching remains low, particularly for carbonatite ores with high calcite content, which hinders leaching efficiency. Hence, this study aims to compare the REEs recovery efficiency of different bacterial cultures, including a mixture of thiobacteria, on two carbonatite-hosted REE deposits.

2. Materials and Methods

2.1 Sample of rare earth element ore

REE ores from two deposits were used: the 15th ore body of the west side of Lugiin Gol (LG) deposit in Khatanbulag soum, Dornogovi province, and the Mushgia Khudag (MK) deposit in Tsogt-Ovoo soum, Umnugovi province. After crushing the ores to sizes smaller than 12.5 mm, they were sieved into size fractions as <0.074 mm, 0.1-1.0 mm, 1.0-2.0 mm, 2.0-3.0 mm, 4.0-5.0 and 6.0-12.5 mm for leaching.

2.2 Microorganism and culture medium

For REEs bioleaching, a mixed thiobacteria culture grown in 9 K nutrient medium, including *Thiobacillus denitrificans* (Genbank: OR053813.1) and *Bacillus cereus* (Genbank: OR053804.1), was used. The bacteria were isolated from high-grade chalcopyrite copper ore. After successive transfers in liquid nutrient medium, colonies were isolated on solid nutrient medium to obtain pure cultures. The purity of the bacterial colonies and morphology of the bacterial cells were monitored using an optical microscope (BEL Photonics, BEL Engineering). DNA was extracted using standard methods, amplified using 16S rRNA universal primers 27F (5′-AGAGTTTGATCCTGGCTCAG-3′) and 1492R (5′-TACGGYTACCTTGTTACGACTT-3′), and analyzed via gel electrophoresis by running them on a 2.0% agarose gel.

The 9 K nutrient medium used for the bioleaching process consisted of two separate components: nutrient medium 1, which contains essential micronutrients for the microorganisms ($(NH_4)_2SO_4$ – 3 g/L, KH_2PO_4 – 0.1 g/L, $MgSO_4$ – 0.5 g/L, KCl – 0.1 g/L, $Ca(NO_3)_2$ – 0.013 g/L), and nutrient medium 2, which includes Fe^{2+} as a source of iron ($FeSO_4 \times 7H_2O$ – 44.2 g/L, 3M H_2SO_4 – 5 mL) (Muddanna & Baral, 2021; Silverman & Lundgren, 1959). The 9 K nutrient medium was prepared by sterilizing nutrient medium 1 (containing essential micronutrients) and nutrient medium 2, separately. Nutrient medium 1 is sterilized at 1 atm pressure and 121°C for 15 minutes, while nutrient medium 2 is sterilized at 0.4 atm pressure and 100°C for 10 minutes. Sterile nutrient mediums 1 and 2 are then mixed in a 7:3 (by volume) ratio to prepare the 9 K nutrient medium. Cultures grown in this 9 K nutrient medium for 4 days at a constant temperature of 25°C in an incubator were used for further leaching process.

To determine bacterial cell counts and isolate pure cultures, meat peptone agar was prepared by dissolving 29 grams of dry medium in 1 liter of distilled water, followed by sterilization at 121°C under 1 atm pressure for 15 minutes.

To study the morphology of the bacteria, a drop of the bacterial solution was placed on a microscope slide, gently heated over an alcohol lamp, and air-dried to prepare the sample. The Gram-staining method was employed to stain the bacterial cell wall (Harley, 2002). The stained sample was then examined under an optical microscope at 800X magnification, and the image was captured (Figure 1). Based on the images obtained from the optical microscope and the cell wall staining, it was observed that the mixed thiobacteria (TD&BC) culture was dominantly composed of Gram-negative, rod-shaped bacteria. Specifically, *Thiobacillus denitrificans* (TD) was identified as Gram-negative and rod-shaped, while *Bacillus cereus* (BC) was identified as Gram-positive and rod-shaped.

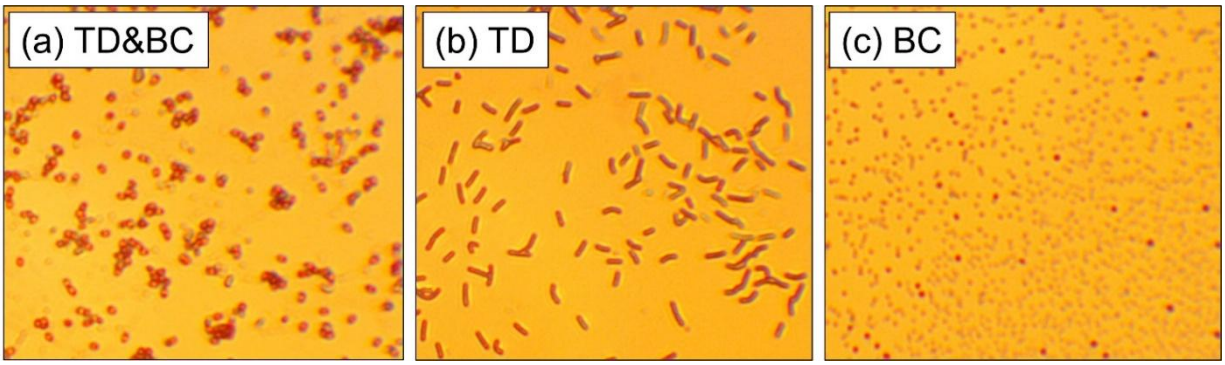

Figure 1. Optical microscopy images of the bacterial culture: a) mixed bacteria, b) *Thiobacillus denitrificans*, c) *Bacillus cereus*

Colony counting on nutrient agar media revealed the following bacterial cell counts: the mixed thiobacteria culture had 2.1×10^6 CFU/mL, *Thiobacillus denitrificans* had 4.5×10^6 CFU/mL, and *Bacillus cereus* had 3.2×10^6 CFU/mL. These counts indicate that the bacterial populations are appropriate for further bioleaching.

2.3 Bioleaching experiment

The bioleaching of REEs was conducted under previously established experimental conditions: a solid-to-liquid ratio of 1:6, shaking speed of 200 rpm, and room temperature for a duration of 7 days, depending on the particle size of the ore (Purevjargal et al., 2023). During the leaching, the pH of the leaching system was measured using a pH meter (PHS-3C precision, Lida), and the oxidation-reduction potential (ORP) was measured using platinum and silver chloride electrodes with a pH/ORP meter (HI9017, Hanna).

The bacterial cell count in the bio-leachate was determined by colony counting on nutrient agar media, both before and after the leaching. The concentration of REEs in the solution was measured using Inductively Coupled Plasma Optical Emission Spectrometry (ICP-OES) with an iCAP 7400 instrument from Thermo Fisher Scientific. Metal recovery was calculated using the following equation:

$$R = \frac{C_M \times V}{m \times w} \times 100\% \quad (1)$$

Where: R is the metal recovery (*%*), C_M *is the concentration of metal in the leachate* (*mg/L*)*; V is the volume of the leachate* (*L*)*; m is the metal mass of ore* (*g*)*; w is the metal concentration in the ore* (*mg/g*).

2.4 Chemical analysis

To perform the chemical analysis of the initial sample, 0.5 ± 0.0001 g of the sample was weighed, and a dissolution was carried out using a mixture of four acids: hydrochloric acid (HCl), nitric acid (HNO_3), perchloric acid ($HClO_4$), and hydrofluoric acid (HF). All reagents used in this experiment were of analytical grade, produced by Unionlab Co. Ltd. (Shanghai, China). For the determination of REEs content, a combined method of alkaline roasting and acid leaching was employed to transfer the elements into the solution. The concentration of REEs was then measured using ICP-OES.

2.5 X-ray diffraction analysis

X-ray diffraction (XRD) patterns of the initial ore sample and the solid residues after leaching were collected using a Shimadzu Maxima X7000 X-ray diffractometer with a Cu Kα radiation source (λ = 0.15418 nm) at a step size of 0.05°. Solid phases were identified using Match! software program, which was utilized to analyze the XRD patterns. The software extracted and

compared the patterns against reference data from the International Centre for Diffraction Data and the RRUFF project databases for accurate phase identification.

3. Results and discussion

3.1 Characterization of initial ore

The macro and microelement content of the REE ores from LG and MK deposits were determined, with the results presented in Table 1 and Table 2 Both LG and MK ores primarily contain CaO 36.96% and 26.03%, respectively, along with significant amounts of carbon dioxide 27.90% in LG and 4.54% in MK and SiO_2 11.28% in LG and 26.97% in MK. Additionally, MK ore contains 15.29% P_2O_5 and 10.74% Fe_2O_3 (Table 1). Compared to the MK ore, the LG ore has 6.14 times more CO_2 and 17.5 times more MnO. Conversely, the MK ore contains 2.39 times more Fe_2O_3 and 37.3 times more P_2O_5 than the LG ore. Both REE ores from LG and MK predominantly contain light rare earth elements such as La, Ce, Nd, Pr, and Sm, along with trace elements like Pb, Zn, and Sr (Table 2). The LG ore had a total REE content of 3.99%, while the MK ore had a total REE content of 7.66% in carbonatite rock. Chemical analysis indicates that these ores are carbonate rock types of rich in light rare earth elements, consistent with the characteristics of carbonatite deposits (Dostal & Gerel, 2023).

Table 1 Initial content of macro- and microelements in REE ores of LG and MK, wt%

Element	SiO_2	Al_2O_3	CaO	MgO	TFe_2O_3	TiO_2	K_2O	Na_2O	MnO	P_2O_5	CO_2	LOI*
LG	11.28	2.54	36.96	1.86	4.68	0.44	1.32	0.33	3.87	0.41	27.90	28.10
MK	26.97	1.67	26.03	0.50	10.74	0.28	0.72	1.96	0.22	15.29	4.54	5.90

**Loss on ignition*

Table 2 Initial content of micro- and rare earth elements in REE ores, mg/kg

	Zr	Ni	Pb	Se	Sr	Ta	Te	V	Zn	Cd	Co	Cu
LG	84.82	18.96	933.1	23.07	5057	30.47	53.02	53.16	582.1	1.14	9.41	38.24
MK	120.7	30.07	270.2	75.77	25288	137.2	181.3	162.9	408.3	1.58	14.82	58.99

	La	Ce	Pr	Nd	Sm	Eu	Gd	Tb
LG	13,434	18,421	1,638	4,787	532.6	92.39	307.1	42.86
MK	25,780	31,190	7,274	9,241	991.8	137.2	277.9	47.85

	Dy	Er	Hf	Yb	Lu	Y	Nb	Tm
LG	50.28	54.57	1.46	21.21	3.1	299.3	50.47	283.6
MK	606.9	144.5	26.42	46.8	7.87	856.7	75.75	<2.0

In addition to chemical analysis, XRD is essential for identifying the mineralogical composition of ores, which provides critical insights into their leaching behavior and overall processing efficiency. The XRD patterns for the two ores used in the study are shown in Figure 2.

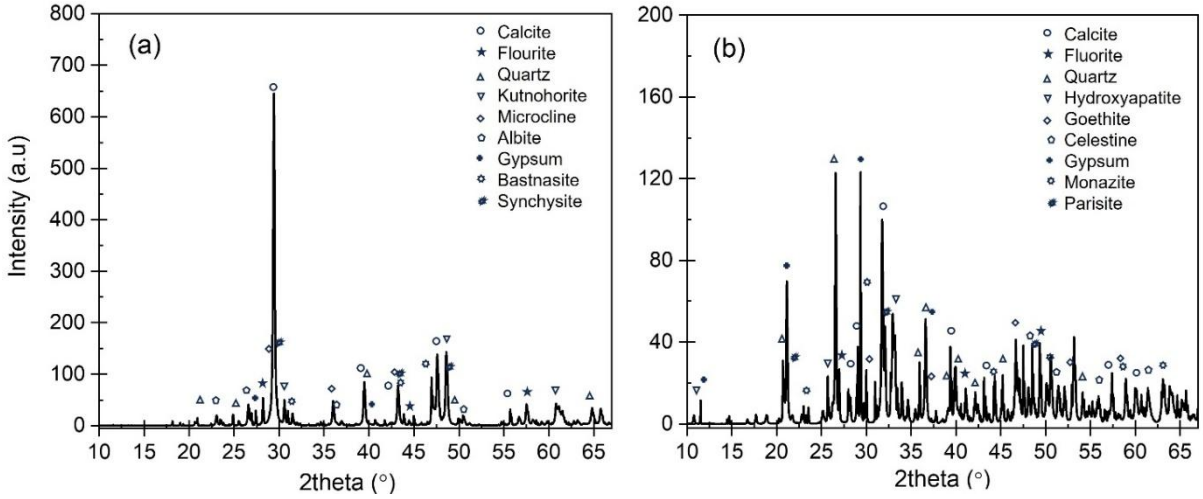

Figure 2. X-ray diffraction patterns of initial REE ores: a) LG, b) MK

The XRD analysis of the ores confirmed the presence of various mineral phases, consistent with the chemical analysis results. In the LG sample (Fa), peaks corresponding to minerals such as calcite ($CaCO_3$), fluorite (CaF_2), quartz (SiO_2), kutnohorite ($Ca(Mn,Mg,Fe)(CO_3)_2$), microcline ($KAlSi_3O_8$), albite ($NaAlSi_3O_8$), and gypsum ($CaSO_4 \cdot 2H_2O$) were observed. In contrast, the MK ore (Fb) showed peaks for hydroxyapatite ($Ca_5(PO_4)_3OH$), quartz (SiO_2), calcite ($CaCO_3$), goethite (FeOOH), celestine ($SrSO_4$), along with fluorite (CaF_2) and gypsum ($CaSO_4 \cdot 2H_2O$). The predominance of carbonate, silicate, phosphate, iron, and calcium-containing minerals in these ores corroborates the findings from the chemical analysis (Table 1). The high calcite and gypsum content could hinder the leaching of REEs by increasing reagent consumption, thereby complicating the extraction. Specifically, bastnasite and synchysite were identified in the LG ore, while monazite and parisite were found in the MK ore (F). These REE-bearing minerals are typically associated with carbonatite rocks and are often spatially or genetically related, in line with observations made by Dostal and Gerel (Dostal & Gerel, 2023).

3.2 Bioleaching of REE ores

To evaluate the effectiveness of the bioleaching using individual bacterial strains TD, BC, and a mixed culture of TD&BC, experiments were conducted on LG and MK ores at room temperature over a 7-day period. The bioleaching efficiency was determined based on the concentration of REEs released into the aqueous media. REEs metal recoveries were calculated using (Eq.1).

The results, summarized in Figure 3, compare the effectiveness of the different bacterial cultures in extracting REEs from the two ores. The figure highlights variations in metal recovery depending on the bacterial culture and ore type. Overall, the mixed TD&BC culture achieved the highest recovery, with significant differences in efficiency observed between the two ores, underscoring the influence of bacterial synergy in enhancing REEs bioleaching.

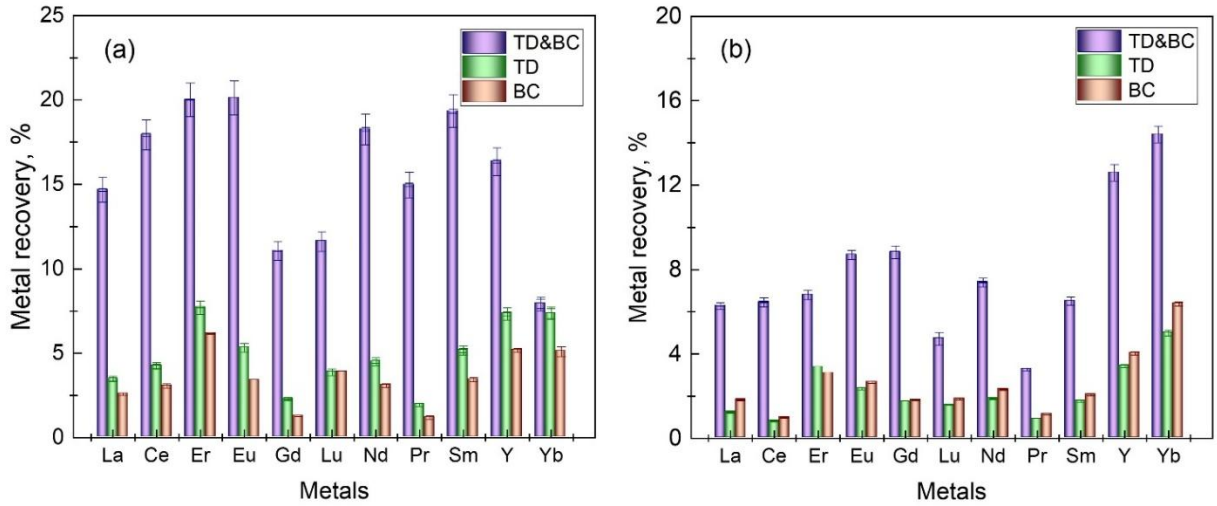

Figure 3. Metal recovery of bioleaching using TD&BC, TD, BC: a) LG, b) MK

The analysis of the overall experimental results revealed that the TD&BC achieved the highest metal recovery, with Eu (20.13%), Er (20.01%), and Sm (19.35%) showing the greatest extraction rates. Among the individual bacterial strains, TD was most effective for Er (7.69%), Y (7.33%), and Yb (7.35%), while BC demonstrated the highest leaching percentages for Er (6.15%), Yb (5.09%), and Y (5.17%) (Figure 3a).

For the LG ore, metal recovery ranged from 1.17% to 6.15% for BC, 1.94% to 7.69% for TD, and 7.92% to 20.13% for the TD&BC. In the case of the MK ore, the TD&BC also achieved the highest metal recovery, with Gd (8.81%), Y (12.58%), and Yb (14.39%). When using individual bacteria, TD and BC resulted in high metal recovery for Er (3.36% and 3.07%), Y (3.41% and 4.02%), and Yb (4.99% and 6.36%) (Figure 3). Total REE recovery for MK ore ranged from 0.98% to 6.23% for BC, 0.81% to 4.99% for TD, and 3.26% to 15.85% for the TD&BC.

Overall, for both LG and MK ores, the highest metal recovery was obtained using the TD&BC, with metal recovery of 15.85% for LG ore and 6.23% for MK ore. This highlights the advantages of employing mixed bacterial cultures in bioleaching for REEs extraction. These findings suggest that the REEs in the LG ore may have been more readily released by bacterial influence, leading to improved leaching efficiency. The leaching efficiency of REEs for the LG ore followed the order: TD&BC > TD > BC, while for the MK ore, the efficiency order was TD&BC > BC > TD.

In addition to REEs leaching, copper recovery in both systems was notably high, reaching 81% and 87% with the mixed bacterial culture. This result aligns with the known effectiveness of TD in copper leaching, as previously demonstrated (Watling, 2006b).

The particle size of the ore plays a critical role in the leaching process by influencing the available surface area for interaction with the leaching solution. Our previous study on the acid leaching of LG ore demonstrated that particle size significantly affects the surface charge of the ore, thereby impacting leaching efficiency. Based on these findings, bioleaching experiments were conducted at room temperature, taking into account the particle size distributions of both the LG and MK ores (Figure 4).

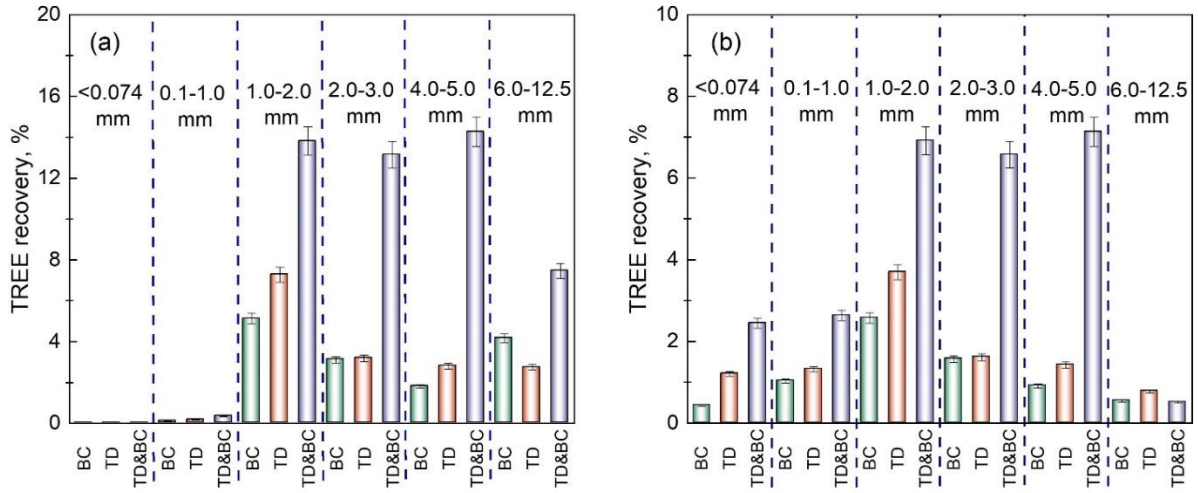

Figure 4. Effect of particle size on bioleaching using TD&BC, TD and BC: a) LG, b) MK

When the particle size of the ore was increased from 0.074 mm to 4.0–5.0 mm, the total REE recovery across all three leaching systems showed a similar trend of increasing recovery. However, when the particle size was further increased to 6.0–12.5 mm, the recovery decreased. This decline can be attributed to the reduced surface area of larger particles, which limits the interaction between the solid and liquid phases. Even though smaller particle sizes (<0.074 mm and 0.1–1.0 mm) offer a larger surface area, the metal recovery remained low.

The highest total REE recovery was observed with particle sizes between 2.0–3.0 mm and 4.0–5.0 mm, achieving 13.1%-14.2% for the LG ore and 6.5%-7.1% for the MK ore. This suggests that an optimal particle size promotes more effective interactions, allowing the ore particles to fully engage with the leaching system (Ruan et al., 2019). At this optimal size, the surface area of the ore is sufficiently exposed, enabling the leaching of the host rock and the subsequent release of REEs into the liquid phase, thereby enhancing the leaching process.

The use of TD&BC resulted in the highest metal recovery, reaching 14.26% for the LG ore (Figure 4a) and 7.10% for the MK ore (Figure 4b) at a particle size of 4.0–5.0 mm. In comparison, the total REEs recovery for the LG ore was roughly twice that of the MK ore when using pure cultures of TD and BC. This indicates that the mixed bacterial culture was more effective in bioleaching than the pure bacterial strains. The mixed culture likely induces a synergistic effect among the microorganisms, enhancing the leaching process for REEs (Fathollahzadeh et al., 2018; Owusu-Fordjour & Yang, 2023; Zhao, He, Qiu, Zhang, & Lin, 2023).

After completing the bioleaching experiments, the solid residues were analyzed using XRD. The results of this analysis are summarized in Figure 5.

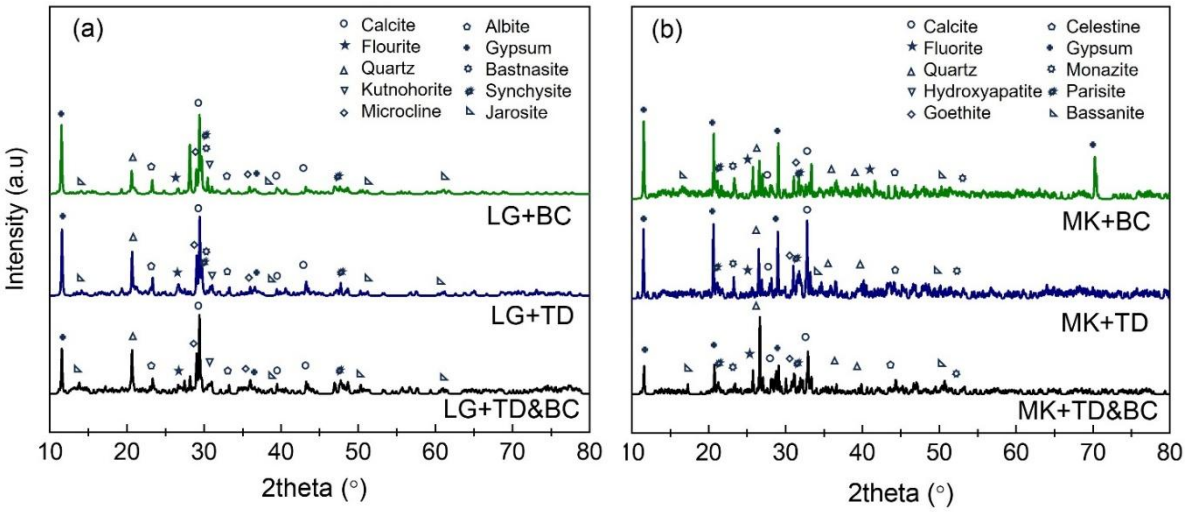

Figure 5. XRD pattern of solid residue after bioleaching: a) LG, b) MK ore

After bioleaching, a notable decrease in the intensity of peaks corresponding to calcite, synchysite, and bastnasite was observed in the LG ore compared to the initial ore (Figure 5a). Similarly, in the MK ore, a reduction in peak intensity was noted for calcite, monazite and parisite (Figure 5b). In contrast, the intensity of gypsum peaks increased. This increase is attributed to the formation of additional gypsum as a result of the leaching of calcite in the ore, as described by the following equation (Eq. 2).

$$CaCO_3 + 2H^+ + SO_4^{2-} + H_2O \rightarrow CaSO_4 \cdot 2H_2O + CO_2\uparrow \quad (2)$$

In the solid residue after bioleaching, the formation of jarosite ($KFe_3(SO_4)_2(OH)_6$) (Eq.3) was detected in the XRD pattern, attributed to the interaction of Fe^{3+} and SO_4^{2-} ions produced by the microbial action (Fathollahzadeh et al., 2018). Jarosite forms a passive layer on the surface of ore, which negatively impacts the leaching process by acting as a barrier that hinders further interactions between the ore and the leaching solution (Hong, Huang, Gan, Qiu, & Wang, 2021).

$$K^+ + 3Fe^{3+} + 2SO_4^{2-} + 6H_2O \rightarrow KFe_3(SO_4)_2(OH)_6 + 6H^+ \quad (3)$$

In the solid residue after the bioleaching of the MK ore, the appearance of a new peak for bassanite reflects the formation of calcium ions from the bacterial metabolic processes in the presence of hydronium ions (Eq.4, 5). Bassanite, with higher solubility than gypsum, forms earlier in the solution and may subsequently transfer into gypsum during the leaching process (Eq.6) (Van Driessche, Stawski, & Kellermeier, 2019).

$$CaCO_3 + 2H^+ \rightarrow Ca^{2+} + H_2O + CO_2 \quad (4)$$

$$Ca^{2+} + SO_4^{2-} + 0.5H_2O \rightarrow CaSO_4 \cdot 0.5H_2O \quad (5)$$

$$CaSO_4 \cdot 0.5H_2O + 1.5H_2O \rightarrow CaSO_4 \cdot 2H_2O \quad (6)$$

The decrease in peak intensities of synchysite, bastnasite, monazite, and parisite in both LG and MK ores after leaching with the TD&BC bacteria indicates that bacterial activity facilitated the leaching of calcite, which hosts these minerals (Eq.2). The bioleaching weakens the associated rare earth minerals including synchysite, bastnasite, monazite, parisite, leading to enhanced leaching efficiency.

The pH of the solution plays a critical role in the bioleaching process, as leaching efficiency tends to improve in acidic conditions. This is particularly significant because the bacteria used in bioleaching generally thrive in acidic environments. During the bioleaching of REEs, both the pH and ORP of the solution were monitored with respect to ore particle size, and the results are summarized in Figure 6.

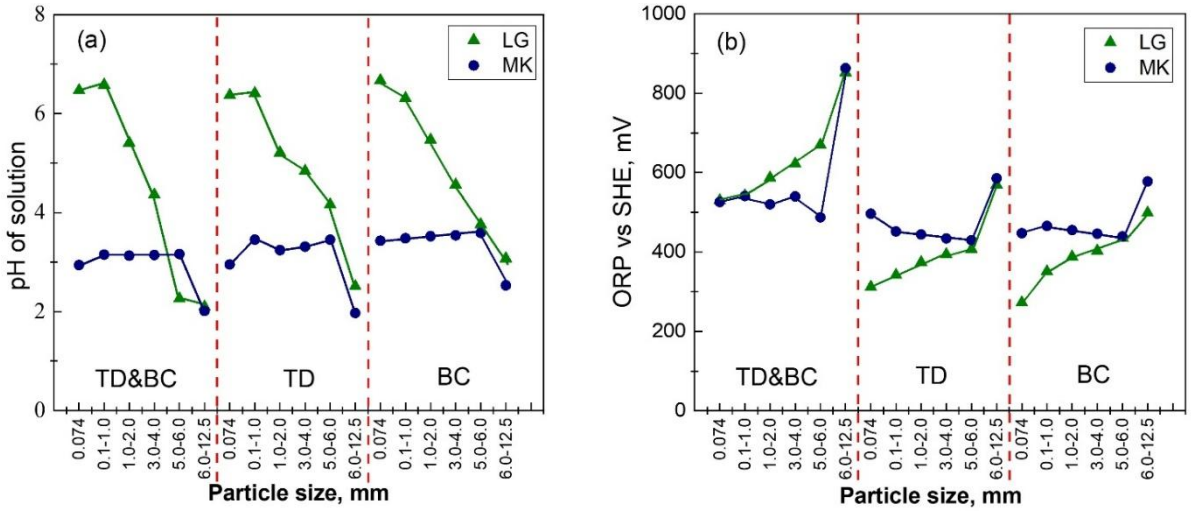

Figure 6. Graphs of the a) pH of the solution and b) ORP against particle size of ore using TD&BC, TD and BC

The observations on pH and ORP changes during the bioleaching process offer valuable insights into the role of ore particle size and its effect on leaching efficiency. The data suggest a strong interplay between the physical behavior of the ore and microbial activity, as seen through variations in pH and ORP.

For the LG ore, the higher pH observed with smaller particle sizes likely reflects the more effective leaching of calcite and other minerals, which can neutralize some of the acids produced during bioleaching. This neutralization raises the pH of the solution, as depicted in Figa. Conversely, larger particle sizes result in less effective leaching due to reduced surface area for microbial interaction, leading to lower pH values and diminished leaching efficiency.

In contrast, the MK ore shows a more stable pH profile, remaining relatively unchanged until the particle size reaches 6.0–12.5 mm, at which point the pH drops sharply. This is likely due to the increased surface area with smaller particle sizes, which facilitates the leaching of calcite and the interaction of ore particles with hydronium ions produced during the metabolic processes of thiobacteria (Eq 4 and 5, Figure 6a). The lower pH during MK bioleaching, compared to LG, highlights the impact of ore composition and mineral interaction on the leaching.

The relationship between ore particle size, pH, and ORP during bioleaching is crucial for understanding the leaching efficiency of REEs. As the ore particle size increases, the pH tends to decrease due to a reduction in the surface area available for interaction with the leaching solution, leading to weaker interactions with calcite. Although a low pH persists with larger particle sizes, the limited contact area between the solid and liquid phases ultimately results in poor REEs recovery.

Conversely, smaller particle sizes result in a lower ORP, ranging from 447 to 525 mV, while larger particle sizes elevate the ORP to between 577 and 863 mV (Figure 6b). This indicates a predominance of reduced ion species in the bioleaching system when the particle size is small, whereas oxidized species become more dominant with larger particles. According to the Eh-pH diagram, REEs typically exist in ionic form when the pH is low (pH < 6.0) and the ORP is high (Eh > 200 mV) (Douglas G.Brookins, 1988; Kim & Osseo-Asare, 2012). Consequently, in our bioleaching system, when the ore particle size is between 1 and 6 mm, lanthanum and cerium are presumably predominantly present in the solution as La^{3+} and Ce^{3+} ions (Al-Nafai, Kim, & Osseo-Asare, 2019), enhancing the effectiveness of the bioleaching.

REEs leaching can occur via several mechanisms: proton-promoted leaching (acidolysis), redox reaction-promoted leaching (redoxolysis), and complexation-promoted leaching

(complexolysis) (Owusu-Fordjour & Yang, 2023). Given these mechanisms, it can be concluded that in the presence of TD&BC cultures, REEs are primarily leached through proton-promoted leaching. The synergistic effect of TD and BC likely enhances this process, making it more efficient than using individual bacterial strains. This highlights the importance of optimizing both microbial cultures and ore particle size for effective bioleaching of REEs.

4. Conclusions

In this study, we isolated *Thiobacillus denitrificans* and *Bacillus cereus* from high-grade chalcopyrite copper ores and utilized them in the bioleaching of REEs. The bioleaching of light REEs-dominant ores from the LG and MK deposits yielded metal extractions of 15.85% and 6.23%, respectively, when employing the TD&BC culture. The use of this mixed culture demonstrated a significant synergistic effect, resulting in enhanced productivity compared to the application of pure bacterial strains. This increase in REEs leaching efficiency under mild conditions underscores the potential for developing economically viable technologies for REEs extraction. Since the bioleaching effectively liberates REEs associated with ore minerals, there is a promising opportunity to integrate this process with acid or other leaching methods, potentially utilizing it as a pre-treatment step in mineral processing. Overall, our findings highlight the effectiveness of TD&BC cultures in bioleaching applications and pave the way for further research into optimizing this approach for rare earth elements recovery.

Acknowledgements

This research was supported by the joint project between Mongolian Foundation for Science and Technology and Ministry of Science and Technology of China (CHN-2022/272).

Compliance with Ethical Standards

Conflict of interest. The authors declare that there is no conflict of interest.

Reference

[1]. Al-Nafai, I., Kim, H., & Osseo-Asare, K. (2019). Estimation of the Standard Free Energy of Formation of Bastnasite, $REFCO_3$. *Mining, Metallurgy and Exploration*, *36*(1), 227–233. https://doi.org/10.1007/s42461-018-0041-7

[2]. Brisson, V. L., Zhuang, W.-Q., & Alvarez-Cohen, L. (2016). Bioleaching of rare earth elements from monazite sand; Bioleaching of rare earth elements from monazite sand. *Biotechnol. Bioeng*, *113*, 339–348. https://doi.org/10.1002/bit.25823/abstract

[3]. Corbett, M. K., Gifford, A., Fimognari, N., & Watkin, E. L. J. (2024). Analysis of element yield, bacterial community structure and the impact of carbon sources for bioleaching rare earth elements from high grade monazite. *Research in Microbiology*, *175*(1–2), 104133. https://doi.org/10.1016/j.resmic.2023.104133

[4]. Dostal, J., & Gerel, O. (2023). Rare Earth Element Deposits in Mongolia. *Minerals*, *13*(1), 129. https://doi.org/10.3390/min13010129

[5]. Douglas G.Brookins. (1988). *Eh-pH Diagrams for Geochemistry*. New York: Springer-Berlag.

[6]. Fathollahzadeh, H., Hackett, M. J., Khaleque, H. N., Eksteen, J. J., Kaksonen, A. H., & Watkin, E. L. J. (2018). Better together: Potential of co-culture microorganisms to enhance bioleaching of rare earth elements from monazite. *Bioresource Technology Reports*, *3*, 109–118. https://doi.org/10.1016/j.biteb.2018.07.003

[7]. Feng, X., Long, Z., Cui, D., Wang, L., Huang, X., & Zhang, G. (2013). Kinetics of rare earth leaching from roasted ore of bastnaesite with sulfuric acid. *Transactions of Nonferrous Metals Society of China*, *23*(3), 849–854. https://doi.org/10.1016/S1003-6326(13)62538-8

[8]. Gonzalez Baez, A., Muñoz, L. P., Timmermans, M. J., Garelick, H., & Purchase, D. (2024). Molding the future: Optimization of bioleaching of rare earth elements from electronic waste by *Penicillium expansum* and insights into its mechanism. *Bioresource Technology*, *402*, 130750. https://doi.org/10.1016/j.biortech.2024.130750

[9]. Halinen, A. K., Rahunen, N., Kaksonen, A. H., & Puhakka, J. A. (2009). Heap bioleaching of a complex sulfide ore. Part I: Effect of pH on metal extraction and microbial composition in pH controlled columns. *Hydrometallurgy*, *98*(1–2), 92–100. https://doi.org/10.1016/j.hydromet.2009.04.005

[10]. Harley, J. (2002). *Laboratory exercise in microbiology* (fifth). McGraw−Hill.

[11]. Hong, M., Huang, X., Gan, X., Qiu, G., & Wang, J. (2021). The use of pyrite to control redox potential to enhance chalcopyrite bioleaching in the presence of *Leptospirillum ferriphilum*. *Minerals Engineering*, *172*, 107145. https://doi.org/10.1016/j.mineng.2021.107145

[12]. Hosseini Nasab, M., Noaparast, M., Abdollahi, H., & Amoozegar, M. A. (2020). Indirect bioleaching of Co and Ni from iron rich laterite ore, using metabolic carboxylic acids generated by *P. putida*, *P. koreensis*, *P. bilaji and A. niger*. *Hydrometallurgy*, *193*, 105309. https://doi.org/10.1016/j.hydromet.2020.105309

[13]. Huang, Y., Dou, Z., Zhang, T., & Liu, J. (2017). Leaching kinetics of rare earth elements and fluoride from mixed rare earth concentrate after roasting with calcium hydroxide and sodium hydroxide. *Hydrometallurgy*, *173*, 15–21. https://doi.org/10.1016/j.hydromet.2017.07.004

[14]. Huang, Y., Zhang, T., Dou, Z., Liu, J., & Tang, F. (2014). Study on leaching rare earths from bastnaesite treated by calcification transition. *Journal of Rare Earths*, *32*(11), 1043–1047. https://doi.org/10.1016/S1002-0721(14)60181-2

[15]. Kim, E., & Osseo-Asare, K. (2012). Aqueous stability of thorium and rare earth metals in monazite hydrometallurgy: Eh-pH diagrams for the systems Th-, Ce-, La-, Nd-(PO_4)-(SO_4)-H_2O at 25°C. *Hydrometallurgy*, *113–114*, 67–78. https://doi.org/10.1016/j.hydromet.2011.12.007

[16]. Liu, S.-L., Fan, H.-R., Liu, X., Meng, J., Butcher, A. R., Yann, L., Yang, K.-F., & Li, X.-C. (2023). Global rare earth elements projects: New developments and supply chains. *Ore Geology Reviews*, *157*, 105428. https://doi.org/10.1016/j.oregeorev.2023.105428

[17]. Ma, J., Li, S., Wang, J., Jiang, S., Panchal, B., & Sun, Y. (2023). Bioleaching rare earth elements from coal fly ash by *Aspergillus niger*. *Fuel*, *354*, 129387. https://doi.org/10.1016/j.fuel.2023.129387

[18]. Muddanna, M. H., & Baral, S. S. (2021). Bioleaching of rare earth elements from spent fluid catalytic cracking catalyst using *Acidothiobacillus ferrooxidans*. *Journal of Environmental Chemical Engineering*, *9*(1), 104848. https://doi.org/10.1016/j.jece.2020.104848

[19]. Owusu-Fordjour, E. Y., & Yang, X. (2023). Bioleaching of rare earth elements challenges and opportunities: A critical review. *Journal of Environmental Chemical Engineering*, *11*(5), 110413. https://doi.org/10.1016/j.jece.2023.110413

[20]. Purevjargal, D., Bayarbayasgalan, B., Tuul, S., Sukhbaatar, B., Altangerel, A., & Sarangerel, D. (2023). Sequential leaching of the synchysite-bearing ore by sulfuric acid and thio-bacteria. *Bulletin of the Institute of Chemistry and Chemical Technology*, (11), 1–8. https://doi.org/10.5564/bicct.v11i11.3281

[21]. Qu, Y., & Lian, B. (2013). Bioleaching of rare earth and radioactive elements from red mud using Penicillium tricolor RM-10. *Bioresource Technology*, *136*, 16–23. https://doi.org/10.1016/j.biortech.2013.03.070

[22]. Rodríguez, Y. (2003). New information on the sphalerite bioleaching mechanism at low and high temperature. *Hydrometallurgy*, *71*(1–2), 57–66. https://doi.org/10.1016/S0304-386X(03)00174-9

[23]. Ruan, Z., Li, M., Gao, K., Zhang, D., Huang, L., Xu, W., & Liu, X. (2019). Effect of Particle Size Refinement on the Leaching Behavior of Mixed Rare-Earth Concentrate Using Hydrochloric Acid. *ACS Omega*, *4*(6), 9813–9822. https://doi.org/10.1021/acsomega.9b01141

[24]. Santaolalla, A., Gutierrez, J., Gallastegui, G., Barona, A., & Rojo, N. (2021). Immobilization of Acidithiobacillus ferrooxidans in bacterial cellulose for a more sustainable bioleaching process. *Journal of Environmental Chemical Engineering*, *9*(4), 105283. https://doi.org/10.1016/j.jece.2021.105283

[25]. Shen, L., Zhou, H., Shi, Q., Meng, X., Zhao, Y., Qiu, G., Zhang, X., Yu, H., He, X., He, H., & Zhao, H. (2023). Comparative chemical and non-contact bioleaching of ion-adsorption type rare earth ore using ammonium sulfate and metabolites of *Aspergillus niger* and *Yarrowia lipolytica* to rationalise the role of organic acids for sustainable processing. *Hydrometallurgy*, *216*, 106019. https://doi.org/10.1016/j.hydromet.2023.106019

[26]. Shin, D., Kim, J., Kim, B. S., Jeong, J., & Lee, J. C. (2015). Use of phosphate solubilizing bacteria to leach rare earth elements from monazite-bearing ore. *Minerals*, *5*(2), 189–202. https://doi.org/10.3390/min5020189

[27]. Silverman, M. P., & Lundgren, D. G. (1959). Studies on the Chemoautotrophic iron bacterium Ferrobacillus ferrooxidans. *Journal of Bacteriology*, *77*(5), 642–647. https://doi.org/10.1128/jb.77.5.642-647.1959

[28]. Su, H., Chen, H., & Lin, J. (2020). A sequential integration approach using *Aspergillus Niger* to intensify coal fly ash as a rare metal pool. *Fuel*, *270*, 117460. https://doi.org/10.1016/j.fuel.2020.117460

[29]. Van Driessche, A. E. S., Stawski, T. M., & Kellermeier, M. (2019). Calcium sulfate precipitation pathways in natural and engineered environments. *Chemical Geology*, *530*, 119274. https://doi.org/10.1016/j.chemgeo.2019.119274

[30]. Watling, H. R. (2006a). The bioleaching of sulphide minerals with emphasis on copper sulphides - A review. *Hydrometallurgy*, *84*(1–2), 81–108. https://doi.org/10.1016/j.hydromet.2006.05.001

[31]. Watling, H. R. (2006b). The bioleaching of sulphide minerals with emphasis on copper sulphides - A review. *Hydrometallurgy*, *84*(1–2), 81–108. https://doi.org/10.1016/j.hydromet.2006.05.001

[32]. Zahiri, A., Ahmadi, A., Foroutan, A., & Ghadiri, M. (2021). Improvement of zinc bioleaching from a zinc flotation concentrate using mechanical activation. *Minerals Engineering*, *163*, 106793. https://doi.org/10.1016/j.mineng.2021.106793

[33]. Zhang, L., Dong, H., Liu, Y., Bian, L., Wang, X., Zhou, Z., & Huang, Y. (2018). Bioleaching of rare earth elements from bastnaesite-bearing rock by actinobacteria. *Chemical Geology*, *483*, 544–557. https://doi.org/10.1016/j.chemgeo.2018.03.023

[34]. Zhao, T., He, L., Qiu, Z., Zhang, Z., & Lin, C. (2023). Synergistic effect between sulfate-reducing bacteria and Shewanella algae on corrosion behavior of 321 stainless steel. *Journal of Materials Research and Technology*, *26*, 4906–4917. https://doi.org/10.1016/j.jmrt.2023.08.237